Available online at www.sciencedirect.com
SCIENCE DIRECT®
Microelectronics Reliability 46 (2006) 317–325
MICROELECTRONICS RELIABILITY
www.elsevier.com/locate/microrel

Single event burnout in power diodes: Mechanisms and models

A.M. Albadri [a,*], R.D. Schrimpf [a], K.F. Galloway [a], D.G. Walker [b]

[a] Department of Electrical Engineering and Computer Science, Vanderbilt University, Nashville, TN 37235, United States
[b] Department of Mechanical Engineering, Vanderbilt University, Nashville, TN 37235, United States

Received 22 March 2005; received in revised form 17 June 2005
Available online 16 August 2005

Abstract

Power electronic devices are susceptible to catastrophic failures when they are exposed to energetic particles; the most serious failure mechanism is single event burnout (SEB). SEB is a widely recognized problem for space applications, but it also may affect devices in terrestrial applications. This phenomenon has been studied in detail for power MOSFETs, but much less is known about the mechanisms responsible for SEB in power diodes. This paper reviews the current state-of-knowledge of power-diode vulnerability to SEB, based on both experimental and simulation results. It is shown that present models are limited by the lack of detailed descriptions of thermal processes that lead to physical failure.

1. Introduction

Power devices (e.g., BJTs, MOSFETs, and diodes) in space, high altitude, and terrestrial systems are vulnerable to destructive single event burnout (SEB) induced by energetic particles [1–4]. SEB was first reported in power MOSFETs, and the failure was attributed to the regenerative feedback mechanism that is due to the turn on of a parasitic transistor when a heavy ion strikes the device in the OFF state [1]. Avalanche-generated holes returning from the base–collector region are the key to sustaining a regenerative feedback process that may lead to a state with simultaneous high current and high voltage. Later, Titus reported burnout failures in bipolar transistors, suggesting that the mechanism is similar to that of power MOSFETs [2]. Numerous studies have been conducted investigating SEB in power MOSFETs and they were reviewed in reference [5]. Subsequently, power diode vulnerability to SEB was reported [3,4]. The SEB mechanism is different for diodes than for bipolar transistors because of the absence of bipolar gain [6].

In this paper, we review the current state-of-knowledge for SEB in power diodes. While the mechanisms responsible for SEB in power MOSFETs are relatively well understood, the processes responsible for power-diode SEB are less clear. The models that have been developed for SEB in power MOSFETs are used to provide a basis for modeling and understanding the basic failure mechanisms in diodes.

2. SEB in power MOSFETS

If a high-energy particle strikes a power MOSFET, it generates electron-hole pairs along its path; as the charges are separated by the electric field, a current is produced. When the charge flows to ground via the

* Corresponding author.
E-mail address: abdulrahman.m.al-badri@vanderbilt.edu (A.M. Albadri).

0026-2714/$ - see front matter © 2005 Published by Elsevier Ltd.
doi:10.1016/j.microrel.2005.06.015

body, the voltage drop in the body resistance may turn on the parasitic bipolar transistor that is an integral part of double diffused MOS (DMOS) power transistors. If the applied voltage is not removed from the device quickly, simultaneous high currents and high voltages induce second breakdown of the parasitic bipolar transistor and can result in meltdown of the device. There have been many models to describe this mechanism [1,7–9]. However, none of these models includes the physical destruction of the device caused by thermal processes.

Waskiewicz et al. reported the breakdown of power MOSFETs under irradiation with ^{252}Cf products [1]. This breakdown was attributed to the turn-on of a parasitic BJT inherent to the MOSFET structure [8]. The failure mechanism was described based on the current induced avalanche (CIA) model [7] as a result of the base push-out phenomenon [10]. Hohl and Johnson proposed a model that explains the regenerative feedback mechanism [11]. This model describes the multiplication factor as the ratio of the generated holes to the injected electrons at the base side of the base–collector depletion region. Using a non-destructive technique, Kuboyama et al. measured the total generated charge of different power MOSFETs exposed to mono-energetic ions [9]. In their measurements, they tested a diode structure, which was fabricated exactly like a MOSFET but without source diffusion. Unlike the MOSFETs, this diode did not undergo SEB. Moreover, the results of the collected charge show two peaks prior to the failure for the MOSFETs in comparison to only one peak for the diode as shown in Fig. 1. The second peak indicates the effect of activating the parasitic BJT.

The experimental and the analytical models provided insight into the failure mechanism and identified the responsible device parameters, specifically the bipolar gain. This helped in paving the way for use of numerical simulation of SEB events to account for the time dependence and investigate the effects of the internal parameters. Roubaud et al. successfully used a TCAD tool to correlate the SEB simulation results with the experimental data [12]. Dachs et al. utilized a 2D device simulator to investigate the ion's impact position effect on SEB in power MOSFETs [13]. They reported that the neck region close to the channel is more sensitive to SEB than regions closer to the source/body contact. This result is attributed to the higher base resistance experienced when the hole current must travel to the body contact through a longer portion of the body. Moreover, the use of device simulation allowed the investigation of hardening solutions [14].

3. SEB in power diodes

Catastrophic failures in power diodes were first reported in 1994 by Kabza et al. [3] and Zeller [4]. The failure was attributed to a localized breakdown in the bulk of the device. Kabza et al. conducted a field experiment using eighteen diodes placed in different environments [3]. They first tested the diodes when they were placed in a tin roofed laboratory. Failure events were recorded as shown in Fig. 2, which illustrates the number of failures vs. time. The diodes were then moved into a salt mine 140 m below ground after replacing the damaged devices. During 6000 device hours, no failure was recorded. The same diodes were taken to the laboratory again and the failures occurred with the same rate as in the first stage of the experiment. To investigate the effect of the shielding, the eighteen diodes were placed in a basement with an equivalent shielding of 2.5 m of reinforced concrete. Failures occurred but with lower rates

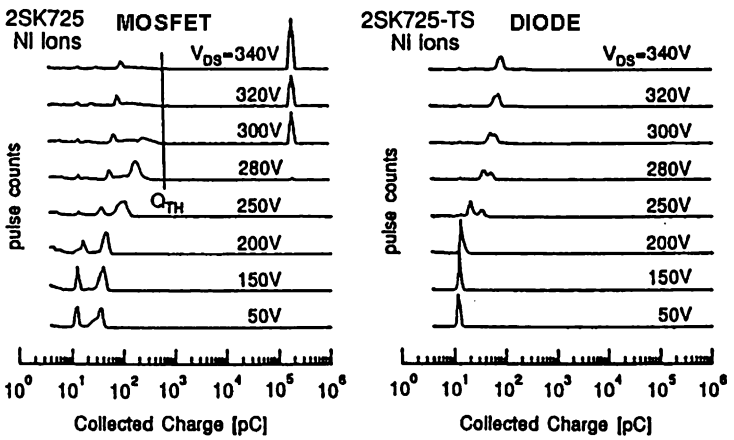

Fig. 1. The collected charge for the MOSFET (2SK725) and the diode (2SK725-TS) when they were exposed to 200 MeV Ni ions (LET=30 MeV/mg/cm^2) (© 1992 IEEE) [9].

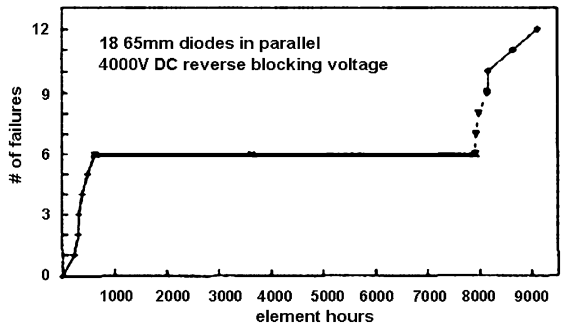

Fig. 2. Device failure versus time for the salt mine experiment (© 1994 IEEE) [3].

compared to the laboratory stage. The shielding effect in this experimentation shows that the failure in power diodes is due to cosmic rays.

Power diodes do not contain an inherent BJT; therefore, the failure mechanism must be different than that described above for power MOSFETs. Previous studies have shown that the direct energy deposition from a high-energy particle crossing the device is insufficient to cause burnout failure [3,15]. It was suggested that a particle-induced nuclear excitation can lead to local field sufficient for impact ionization. In other words, no failure mechanism is triggered unless a particle causes a nuclear reaction with lattice atoms [4,15]. This is in agreement with the observations of burnout failures caused by short range particles, where the deposited energy does not occur at the high electric field regions [15].

Since cosmic rays may cause catastrophic failures through nuclear reactions, i.e., the formation of a cascade of heavier ions such as silicon and aluminum, many studies have approached the failure experimentally by irradiating the power devices with heavy ions that have high values of linear energy transfer (LET) [16]. Irradiation experiments with high energy neutrons and protons have also produced burnout failures in power diodes [17,18]. Preliminary simulations have identified avalanche multiplication of ion-generated carriers as a source of charge that may be involved in the ion-induced breakdown of the device [3,17]. However, in these simulations, once the carriers are removed from the device by the field, the current falls back to zero, and the device recovers.

More recently, experimental and simulation studies have tried to predict and model the burnout of power diodes. Destructive and non-destructive measurements have been used to investigate the burnout process. Non-destructive measurements are only able to indicate the onset of avalanche multiplication. On the other hand, destructive measurements are able to provide more detail about the burnout process. Numerical simulations are required to understand the variation of internal parameters during the burnout mechanism.

3.1. Charge measurements

Avalanche multiplication is believed to be one of the key mechanisms responsible for triggering SEB events in diodes. Therefore, studies have investigated the process leading to charge multiplication in detail using non-destructive charge measurements [6,19]. In the test performed by Maier et al., it is required for the device to be hit by a single ion at a time [6]. This can be achieved by reducing the ion flux below 100 ions/s. The generated charge can be measured with a charge-sensitive preamplifier. Note that surface barrier detectors (SBDs) operate in the same way but at smaller voltages [20]. A typical charge spectrum for charge measurements is shown in Fig. 3 [6]. In this figure, the collected charge of a 4 kV power diode irradiated by 90 MeV Kr ions is shown. At low voltages, below 850 V, a single peak is observed, which corresponds to the direct energy loss of the ion. The peak broadens and shifts to higher charge as the voltage increases. Maier et al. interpreted this shift as a slight amplification of the charge carriers and also as incomplete charge collection at low voltage [6]. A second peak starts to appear at 875 V as a result of avalanche multiplication at high electric fields. It corresponds to a charge increase of about twenty times as seen by taking the ratio of the corresponding charge of the two peaks in the logarithmic scale of the *X*-axis. As voltage continues to increase, the consequent increase of the electric field produces more charge through

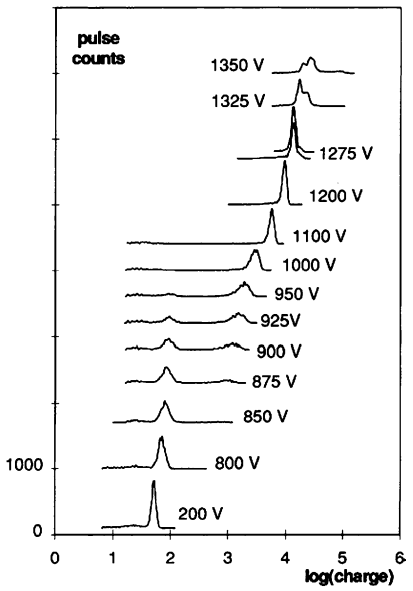

Fig. 3. Charge spectrum from the bombardment of a 4 kV diode with 90 MeV Kr ions showing the number of events as a function of the total generated charge with increasing the applied voltage, reprinted from [6], copyright (1998), with permission from Elsevier.

avalanche multiplication. At 1100 V, the first peak diminishes and all incoming charge undergoes avalanche multiplication.

Similar results have been obtained for the same diode structure with different ions and different energies [6,21]. The generated charge data for Kr, Si, and C ions are summarized in Fig. 4 as a function of the applied voltage. The vertical lines represent the threshold voltage of the multiplication. This steep transition represents the sensitive dependence of generated charge on applied voltage. With Kr irradiation, the multiplication is triggered at relatively low voltages. The generated charge, however, was only a factor of two to ten greater than the radiation-induced charge. For the Si ions, the multiplication set in at higher voltages (1500–1800 V) and the generated charge was higher than the ion-induced charge by a factor of 100–1000. The 17 MeV C data were comparable to the 13.5 MeV Si results. Interestingly, the multiplication is triggered at a higher voltage when the 17 MeV C ions hit the diode at an angle of 30°. It can be concluded from Fig. 4 that heavier ions trigger the multiplication at low voltages. Increasing the ion energy also causes the multiplication to start at lower voltages. Perpendicular strikes trigger the multiplication at lower voltages compared to inclined strikes. As stated above, once the multiplication process is triggered, the amount of the generated charge depends mainly on the applied voltage, and it is independent of the starting event.

Different experimental results showed that the multiplication is triggered at a lower voltage for a lower energy, which are in contradiction to the previous results [16]. These unexpected results are actually attributed to the different penetration depth (range) of the ions as shown in Fig. 5 for a particular diode structure. The Bragg peak of the 108 MeV ions is at 38 μm while it is at 60 μm for the 156 MeV ions. The avalanche multiplication is maximized when the Bragg peak (maximum LET) occurs at a position where the electric field is higher; i.e., the Bragg peaks of 108 and 156 MeV ions coincide with positions where the electric field is 100 and 80 kV/cm, respectively. This indicates that SEB occurrence is dependent on the charge induced in the sensitive (high electric field) region rather than the total ion-deposited charge.

3.2. Current measurements

In this section, we highlight the current waveform outputs during the failure event. By analyzing the real current waveforms during destruction, more details of the physical mechanism can be gained. Soelkner et al. presented a set of current measurements under proton irradiation [17]. Current waveforms were detected using magnetic probe measurement and direct measurement. Fig. 6 shows the transient current output of a 4 kV power diode irradiated with 70 MeV protons. An initial current pulse of 4 A due to avalanche multiplication is followed by a sharp rise in current after about 100 ns. The second rise of the current represents the occurrence of SEB; i.e., the device is destroyed.

Hallen et al. used the Uppsala EN (6 MV) tandem accelerator to study the effect of cosmic rays on a 2.7 kV power diode [22]. The device was exposed to 30 MeV C ions when the reverse voltage was 1.8 or 2 kV. In this experiment, pulses with 3 ms duration time and different number of ions were generated to investigate the effect of changing the ion fluence on failure occurrence. For pulses containing 10^6 ions (flux of 3.33×10^8 ions/cm^2 s), no failure event was observed in

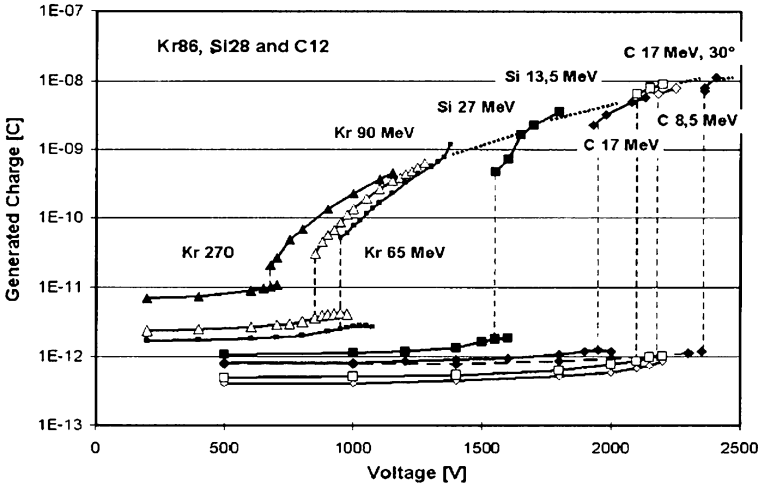

Fig. 4. Summary of results on avalanche multiplication in 4 kV diodes under ion irradiation. Different ions and different energies are presented, reprinted from [21], copyright (2004), with permission from Elsevier.

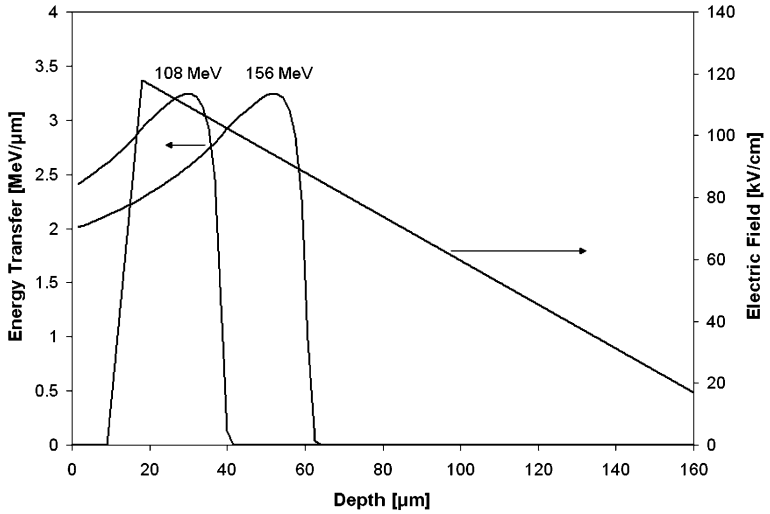

Fig. 5. LET of silicon ions at 108 MeV and 156 MeV inside silicon crystal along with the electric field distribution for a biased voltage of 1000 V. Reproduced after [19].

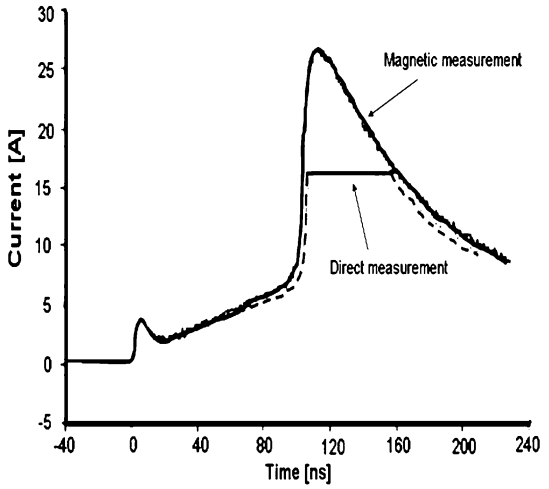

Fig. 6. Current signals of destructive events for 4 kV power diode irradiated with 70 MeV protons (© 2000 IEEE) [17].

the case of 1.8 kV applied voltage. However, at 2 kV a pulse of only 10^4 ions resulted in a failure, which was represented by a sudden increase in the current. The experimental data for different numbers of incident ions at different applied voltages showed that at higher voltages, fewer incident ions are needed to cause a failure. Numerical simulation is needed to reproduce these destructive results so that the full SEB mechanism can be identified.

3.3. Numerical simulation

It is often useful and illuminating to model the electrical characteristics of semiconductor devices using numerical simulation. Transient simulations indeed can account for the time dependence of the mechanisms leading to SEB. 2-D rectangular and 2-D axi-symmetrical diode structures have been simulated in several works [3,17,23,24]. Because of the 3-D nature of the ion strike that makes the mechanism of SEB a 3-D effect, a complete description of the device response would require performing 3-D simulations. The drawback of performing 3-D simulations is the computing resources required. The dense mesh along the ion strike and the very small temporal steps required to resolve the evolution of the charge with time lead to very long computing times.

Simulation models of SEB in power diodes investigate the electrical characteristics by solving Poisson's equation, along with the continuity equations for both electrons and holes. The impact ionization model is very important in describing ion-induced breakdown. Ion-induced charge deposition is modeled with a temporally and spatially localized carrier generation rate.

The first attempt to model SEB of power diodes using numerical simulation was performed by Kabza et al. [3]. They simulated a cylindrical diode by depositing radiation-generated carriers along the center device axis. Their transient simulation shows two peaks of the output current, as shown in Fig. 7. The first peak is a result of the radiation-induced charge collected from the depletion region; thus, its collection is very quick. A second peak, 3 ns later, is attributed to the avalanche-generated charge. The current eventually goes back to zero, so the destructive part of the event is not modeled.

Later simulation models have focused on the temporal and spatial evolution of the internal electric field and the electron density along the incident track. Kaindl

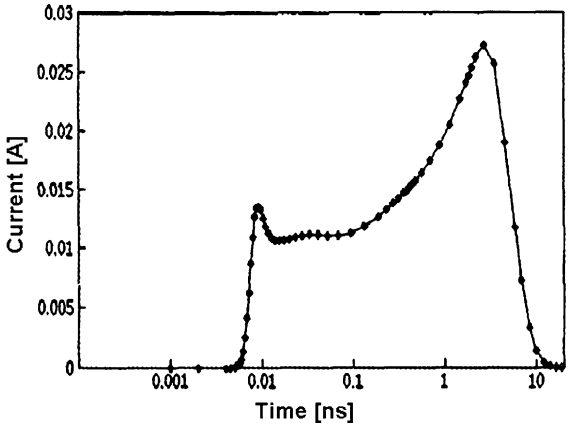

Fig. 7. Simulated current for 5×10^9 carriers generated by a particle (© 1994 IEEE) [3].

et al. studied the charge amplification in power diodes using cylindrically-symmetrical simulations [23]. They modeled a 17 MeV C ion in a 3.5 kV power diode biased at 1900 and 2000 V. Fig. 8 shows the temporal and spatial evolution of the electric field and the electron density along the axis of symmetry. The electric field maximum moves throughout the device while the electron density broadens in response to charge distortion due to the ion strike. In the 1900 V case, the electric field peak diminishes with time and does not support significant avalanche multiplication. Therefore, the collected charge corresponds only to the charge deposited by the ion. On the other hand, for the 2000 V case, the electric field peak moves from the anode to the cathode, resulting in more avalanche-generated charge. This mechanism is similar to the process leading to second breakdown of power diodes when high voltage pulses are applied [25]. The failure due to second breakdown is triggered by the onset of impact ionization at the nn^+ junction, which is analogue to the movement of the electric field peak shown in Fig. 8. The electron density in the 2000 V case becomes large throughout the distance between the anode and the cathode. This event would be considered as the onset of destruction, while a non-destructive event is observed when the applied voltage is 1900 V. These simulation results correlate with experimental data produced by Maier et al. [6].

Kaindl et al. also compared the simulation results of charge multiplication events triggered by ions for two different diode structures: non-punch-through (NPT) diodes and punch-through (PT) diodes [23]. The results indicate that PT diodes are more robust against cosmic

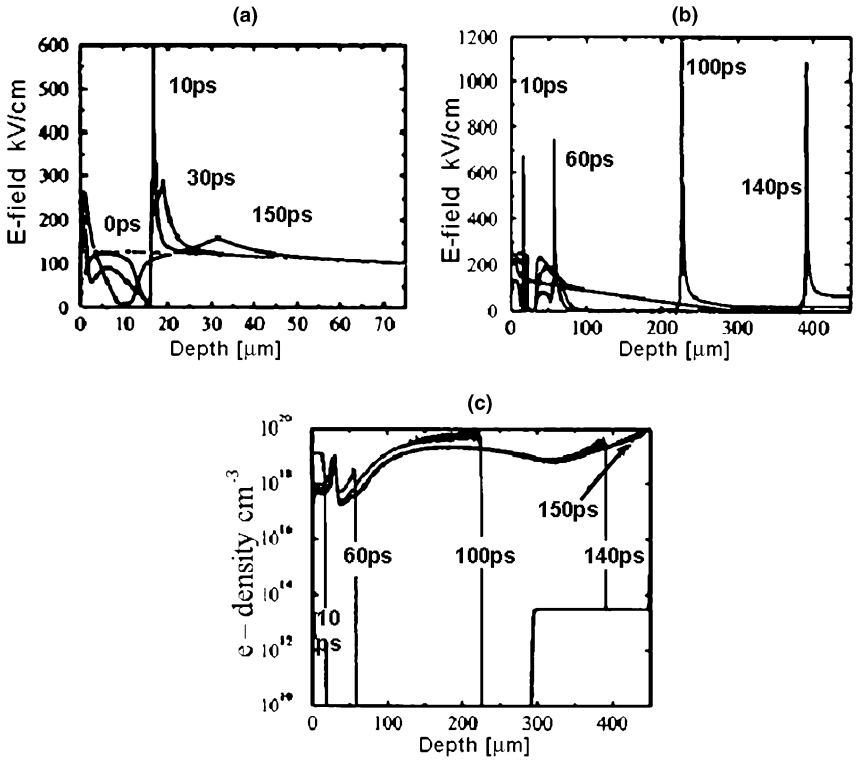

Fig. 8. Simulation of the spatial and temporal evolution of the internal electric field and of the electron density in a 3.5 kV diode, given along the axis of symmetry, for C (17 MeV) irradiation: electric field at a bias of 1900 V (a) and 2000 V (b) electron density at a bias of 2000 V (c) (© 2003 IEEE) [23].

radiation in comparison to NPT diodes. For the simulation results to reproduce the experimental results correctly, the avalanche coefficients need to be re-adjusted when the electric field exceeds 600 kV/cm.

Studies published to date did not simulate the burnout process to the point of failure. It has been suggested that catastrophic failure is a result of self-heating [3]. Strike-induced charge as well as charge multiplication can yield sufficiently large current to generate high local temperatures. In some cases, the temperature can rise above the melting temperature of silicon, resulting in damage. This poses the need for a coupled electro-thermal model that can adequately simulate the burnout mechanism in power devices.

3.4. Non-isothermal simulations

Non-isothermal simulations account for Joule heating that results from large current densities. Non-constant lattice temperature can be considered by adding the thermal diffusion equation to the current electrical models.

$$C_p\rho\frac{\partial T_L}{\partial t} = \nabla\cdot(\kappa\nabla TL) + \vec{J}\cdot\vec{E} \tag{1}$$

where C_p is the specific heat, ρ is the density of the material, T_L is the lattice temperature, κ is the thermal conductivity, and the product of the current density and the electric field ($J{\cdot}E$) represents the heat generation due to Joule heating. Most electrical properties of semiconductor devices are temperature dependent. Therefore, the influence of lattice heating on device characteristics is crucial. As temperature increases, lattice scattering increases. As a result, the mobility decreases and in turn the current density becomes lower. Jacoboni et al. reported that for a 100 °C increase in silicon, mobility will decrease by 20% [26]. In other words, at high electric field, temperature increase limits the carrier velocity. Also, avalanche-generated charge becomes less as temperature increases because of the reduced mean free path. More importantly, as temperature increases, the contribution of thermally generated charge becomes significant. The temperature-dependent carrier concentration for silicon is [10]:

$$n_i(T_L) = \sqrt{N_c N_v}e^{\left(\frac{-E_g}{2k_B T_L}\right)} \tag{2}$$

where T_L, E_g, and k_B are the lattice temperature, the silicon band gap, and the Boltzmann constant, respectively. The quantities N_c and N_v are the effective densities of states at the conduction and valence band edges. Depending on the device structure and the operating conditions, the temperature may reach a value at which thermally generated carriers contribute significantly to the total current. As a result, a thermal regenerative feedback mechanism is triggered, leading to additional local temperature increase.

A recent study presented primary results of coupled electro-thermal simulations of SEB in power diodes [24]. Fig. 9 shows the transient current after an ion strike obtained from non-isothermal simulation compared to isothermal simulation, along with the obtained maximum temperature due to self heating. In the non-isothermal simulation, the sharp decrease in current is a result of the decreasing saturation velocity resulting from high local temperature. After a period of time, the temperature reaches a level at which the intrinsic carrier concentration begins to dominate the contribution to the current. The increased current resulting from the increased charge causes additional self-heating, which completes the feedback mechanism responsible for device failure. In Fig. 9, the current suddenly exceeds the simulator capability to resolve, indicating device failure. At the point of failure, the value of the intrinsic concentration becomes relatively high ($\sim 1\times10^{20}\,\mathrm{cm}^{-3}$). Because of the short heating time, the temperature rise is extremely localized as shown in Fig. 10. In fact, the

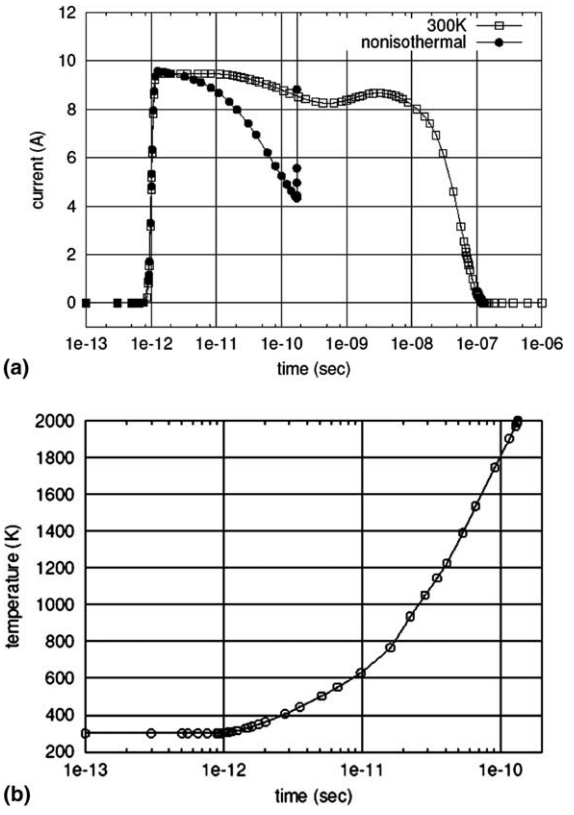

Fig. 9. Output currents of isothermal and non-isothermal simulations with LET = 30 MeV cm^2/mg and $V = 3500$ V, along with the maximum temperature due to self-heating [24].

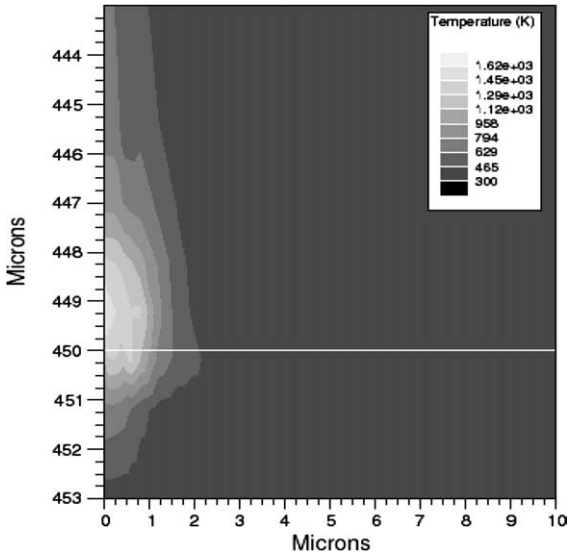

Fig. 10. Temperature distribution near junction at time 100 ps [24].

hot spot extends only 2 μm in the radial direction away from the strike. However, the heating occurs in a region that is approximately 20 μm long in the lightly doped region at the junction. These results demonstrate that simulation of the complete burnout process requires consideration of thermal effects.

In addition, power devices may experience non-equilibrium thermal transport resulting from an ion strike because the time scales involved in burnout failure are of the order of scattering time constants between electrons and phonons. As a result, carriers will not be able to transfer their energy to the lattice atoms efficiently. To account for non-equilibrium effects, the energy balance equation must be utilized. In addition to electrical non-equilibrium, thermal transport is characterized by non-equilibrium as well. Electrons with high kinetic energy (>60 meV) excite optical phonons, which have negligible group velocities; therefore, they are not involved in energy transport. Optical phonons subsequently decay to acoustic phonons, which have large group velocities (7000–8000 m/s in silicon) and are able to transport heat. Because the electron-optical phonon scattering time constant is much shorter than the optical-acoustic phonon decay time, non-equilibrium thermal transport may exist between optical and acoustic phonons. Raman et al. studied non-equilibrium thermal effects in power LDMOS transistors, showing its significant role in transient situations [27]. Non-equilibrium thermal effects associated with ion strikes have been considered to assess the influence of thermal energy in highly scaled devices [28]. Non-equilibrium effects should also be considered to produce a complete description of SEB in power diodes.

4. Conclusions

Power MOSFETs can fail catastrophically when second breakdown is activated as a result of a heavy ion strike. In these devices, a regenerative feedback mechanism must be initiated in order to trigger burnout failure. On the other hand, power diodes ultimately depend on avalanche multiplication to produce SEB. The SEB models published to date do not attempt to describe the entire burnout process, including the eventual failure due to thermal effects. Inclusion of these effects is required to obtain more detailed understanding of the mechanisms responsible for SEB, particularly in power diodes.

References

[1] Waskiewicz AE, Groninger JW, Strahan VH, Long DM. Burnout of power MOS transistors with heavy ions of 252-Cf. IEEE Trans Nucl Sci 1986;33:1710–3.
[2] Titus JL. Single event burnout of power bipolar junction transistors. IEEE Trans Nucl Sci 1991;38:1315–22.
[3] Kabza H, Schulze H-J, Gerstenmaier Y, Voss P, Wilhelmi J, Schmid W, et al. Cosmic radiation as a possible cause for power device failure and possible countermeasures. In: Proceedings of the 6th international symposium on power semiconductor devices & IC's, 9–12, Davos, Switzerland, May 1994.
[4] Zeller HR. Cosmic ray induced failures in high power semiconductor devices. Solid-State Electron 1995;38:2041–6.
[5] Johnson GH, Palau JM, Dachs C, Galloway KF, Schrimpf RD. A review of the techniques used for modeling single-event effects in power MOSFETs. IEEE Trans Nucl Sci 1996;43:546–60.
[6] Maier KH, Denker A, Voss P, Becker H-W. Single-event burnout in high power diodes. Nucl Instrum Methods Phys Res B 1998;146:596–600.
[7] Wrobel T, Beutler D. Solutions to heavy ion induced avalanche burnout in power devices. IEEE Trans Nucl Sci 1992;39:1636–41.
[8] Hohl JH, Galloway KF. Analytical model for single event burnout of power MOSFETs. IEEE Trans Nucl Sci 1987;34:1275–80.
[9] Kuboyama S, Matsuda S, Kanno T. Mechanism for single event burnout of power MOSFETs. IEEE Trans Nucl Sci 1992;39:1698–703.
[10] Baliga BJ. Modern power devices. John Wiley and Sons, Inc.; 1987.
[11] Hohl JH, Johnson GH. Features of the triggering mechanism for single event burnout of power MOSFETS. IEEE Trans Nucl Sci 1989;36:2260–6.
[12] Roubaud Franck, Dachs Charles, Palau Jean-Marie, Gasiot Jean, Tastet Pierre. Experimental and 2D simulation study of the single event burnout in N-channel power MOSFETs. IEEE Trans Nucl Sci 1993;40:1952–8.
[13] Dachs Charles, Roubaud Franck, Palau Jean-Marie, Bruguier Guy, Gasiot Jean. Evidence of the ion's impact

position effect on SEB in n-channel power MOSFETs. IEEE Trans Nucl Sci 1994;41:2167–71.
[14] Dachs Charles, Roubaud Franck, Palau Jean-Marie, Bruguier Guy, Gasiot Jean, Tastet Pierre, et al. Simulation aided hardening of N-channel power MOSFETs to prevent single event burnout. IEEE Trans Nucl Sci 1995;42:1935–9.
[15] Voss P, Maier K, Becker H, Normand E, Wert J, Oberg K, et al. Irradiation experiments with high voltage power devices as a possible means to predict failure rates due to cosmic rays. In: Proceedings of the IEEE international symposium on power semiconductor devices and IC's, 169–173, Weimar, Germany, 1997.
[16] Busatto G, Iannuzzo F, Wyss J, Pantano D, Bisello D. Effects of heavy ion impact on power diodes, radiation and its effects on components and systems, 1999. RADECS 99. In: 1999 fifth european conference on, 13–17 September 1999. p. 205–9.
[17] Soelkner G, Voss P, Kaindl W, Wachutka G, Maier KH, Becker H-W. Charge carrier avalanche multiplication in high-voltage diodes triggered by ionizing radiation. IEEE Trans Nucl Sci 2000;47:2365–72.
[18] Normand E, Wert J, Oberg D, Majewski P. Neutron induced single event burnout in high voltage electronics. IEEE Trans Nucl Sci 1997;44:2358–66.
[19] Busatto G, Iannuzzo F, Velardi F, Wyss J. Non-destructive tester for single event burnout of power diodes. Microelectron Reliab 2001;41:1725–9.
[20] Tsyganov Yu, Kushniruk W, Polyakov A. A look at the phenomenon of charge multiplication in silicon radiation detector within the concept of dynamic focusing of the electric field. IEEE Trans Nucl Sci 1996;43:2496.
[21] Soelkner G, Kaindl W, Schulze H-J, Wachutka G. Reliability of power electronic devices against cosmic radiation-induced failure. Microelectron Reliab 2004;44:1399–406.
[22] Hallen A, Bleichner H, Nordgren K. Cosmic ray induced DC-stability failure in Si diodes, power semiconductor devices and IC's, 1997, ISPSD '97. In: 1997 IEEE international symposium on, 26–29 May 1997. p. 121–4.
[23] Kaindl W, Solkner G, Wachutka G. Analysis of charge carrier multiplication events in NPT and PT-diodes triggered by an ionizing particle, electron devices and solid-state circuits. In: 2003 IEEE conference on, 16–18 December 2003. p. 383–6.
[24] Walker DG, Al-badri AM, Fisher TS, Schrimpf RD. Simulation of single event failure in power diodes. In: Proceedings of IMECE' 02, 17–22, New Orleans, Louisiana, USA, 2002.
[25] Egawa H. Avalanche characteristics and failure mechanism of high voltage diodes. IEEE Trans Electron Dev 1966;13:754–8.
[26] Jacoboni C, Canali C, Ottaviani G, Quaranta A. A review of some charge transport properties of silicon. Solid-State Electron 1977;20:77–89.
[27] Raman A, Walker DG, Fisher TS. Simulation of nonequilibrium thermal effects in power LDMOS transistors. Solid-State Electron 2003;47:1265–73.
[28] Walker DG, Weller RA. Phonon production and nonequilibrium transport from ion strikes. IEEE Trans Nucl Sci 2004;51:3318–23.